African Journal of Environmental Science and Technology Vol. 5(7), pp. 553-566, July, 2011
Available online at http://www.academicjournals.org/AJEST
ISSN 1996-0786 ©2011 Academic Journals

Full Length Research Paper

Evaluation of electrical resistivity anisotropy in geological mapping: A case study of Odo Ara, West Central Nigeria

P. I. Olasehinde[1] and O. O. Bayewu[2]*

[1]Department of Geology, Federal University of Technology, Minna, Niger State, Nigeria.
[2]Department of Earth Sciences, Olabisi Onabanjo University, Ago-Iwoye, Ogun State, Nigeria.

Accepted 8 June, 2011

The study of electrical resistivity anisotropy in rocks has become important in increasing the accuracy of geological mapping using electrical resistivity survey. The study area, Odo Ara near Egbe, west central Nigeria, has been surveyed using electrical resistivity soundings. Sixty Radial Vertical Electrical sounding (RVES) measurements were carried out in the study area which comprises of the banded gneiss, amphibolites, schist and intrusive pegmatites. The aim of the study is to use the electrical resistivity anisotropy properties of the area to resolve its geological setup. The VES data showed a significant presence of electrical resistivity anisotropy. The VES curves obtained were predominantly of 3 geoelectric layer of H-type ($\rho_1>\rho_2<\rho_3$) curves; the topsoil, sandy clay/ clay layer and fractured basement. The pseudo-sections show a good correlation with the geoelectric section. Moreover, the iso-resistivity and isopach maps also show a significant correlation with the lithological and strike of the rocks in the area but due to the non uniqueness of electrical resistivity, the lithologic difference between the banded gneiss and the amphibolite at the south western part of the area could not be totally resolved. However, the combination of the anisotropy polygons and the iso-resistivity map has reduced the ambiguity inherent in using a single geophysical parameter.

Key words: Electrical resistivity anisotropy, radial vertical electrical sounding, anisotropy polygons.

INTRODUCTION

The geological mapping in the Precambrian, to Early Palaeozoic, crystalline, basement complex terrain of Nigeria, which the study area belongs to, poses a lot of problems due to the poor exposure of its outcrop, as a result of the relatively thick overburden (Annor et al., 1990). Different authors have shown the usefulness of electrical resistivity survey in the geological interpretation of the Nigeria Basement complex (Olayinka, 1999; Okurumeh and Olayinka, 1998; Olasehinde, 1984; Olorunfemi and Okhue, 1992). However, apart from problems of equivalence and suppression which cause ambiguities in this interpretation (David, 1994; Zohdy, 1974), the use of electrical resistivity survey has been helpful in unravelling the geology of an area since resistivity values have larger applications compared to other physical quantities mapped by other geophysical methods.

The resistivity of rocks and soils in a survey area can vary by several orders of magnitude, in comparison, density values used in gravity surveys usually change by less than a factor of 2, and seismic velocities usually do not change by more than a factor of 10. This makes the resistivity and other electrical or electromagnetic based methods very versatile geophysical techniques (Loke and Barker, 1996).

In this study, an attempt has been made to use the electrical resistivity anisotropic characteristics of rocks to map lithologic and structural trend of the area.

METHODOLOGY

Study area

The study area is located in Odo Ara, west central part of Nigeria. It lies between longitudes 5°36.0' and 5°37.4' E and latitudes8°14.70' and 8°15.70' N. The area of study is approximately 4.69 km^2 while

*Corresponding author. E-mail: tejubpositive@yahoo.com.

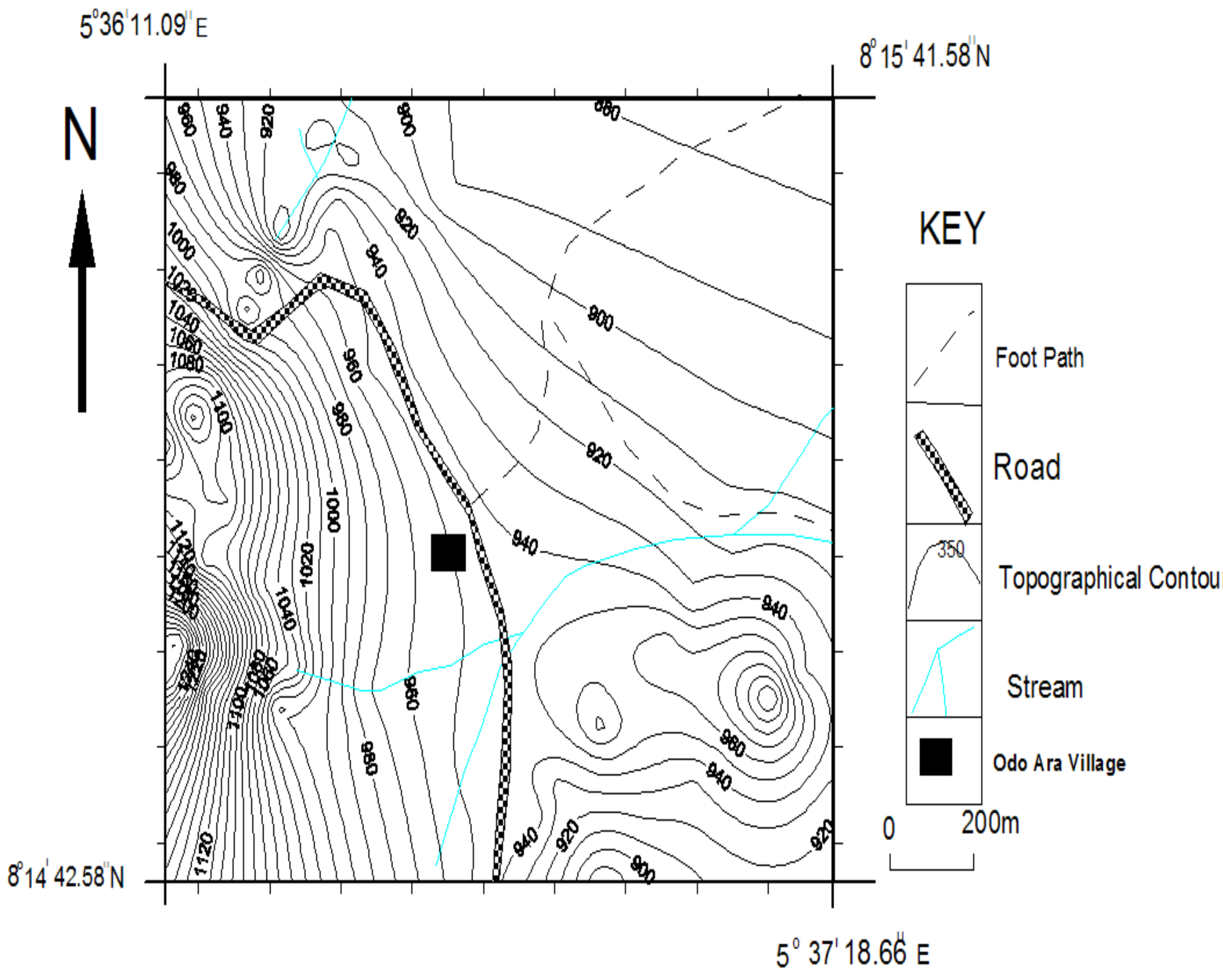

Figure 1. The topographic map of the study area.

the geophysical profiles occupy an area of about 2 km^2 within the area (Figure 1).

The area has a typical savannah climate with distinct wet and dry seasons: a dry season which usually last from December to March and a rainy season which last from April to October. Temperatures vary between 15℃ around December/January and 32℃ in March/April. Average annual rainfall for a thirty year record in the area is about 1270 mm. The annual potential evapo-transpiration calculated using Thonthwaite`s method is 767.2 (Eduvie, 1991).

Geology of the study area

Odo Ara area lies within the Basement Complex terrain of Nigeria. The Nigerian Precambrian basement rocks are loosely categorized into four main lithologic units. They are: The ancient gneiss-migmatite complex with ages ranging from mainly Liberian (ca 2800Ma) to Pan African (600 Ma); older dates (>3000 Ma) have lately been obtained from some of the areas. This is also known as Shamrian Orogeny (Dada et al., 1993; Dada, 2006).

The schist belts, which are generally low grade (green schist facies) meta-sediments which show prominently distinctive structural petrologically and sometimes metallogenic features, occur more prominently in N-S and NNE and SSW direction. They are mainly metamorphosed semi-pelitic assemblage.

Syntectonic to late tectonic granitoids commonly refer to the older granites, intruded both the migmatite gneiss complex and the Schist belts.

The pegmatites, both rare metal and non rare metal-bearing which are thought to be late Pan African intrusive of the older Granites suite intruded the gneisses, schists and Pan African granite and had been hitherto thought to be concentrated in a 400 km long NE-SW trending belt extending from Ijebu area in the Southwest to Wemba-Jemaa area (North Central) and Zuru-Gusau area in the North west. However, prominent occurrences have been revealed around Obalinku (Oban Massif) and Obudu area in the South-eastern sector (Okunola, 1998).

The study area is part of the schist belt of Nigeria and it comprises of three main rock types; the banded gneiss, amphibolite and schist and these rocks have been cross cut by quartz veins and pegmatites (Figure 2).

The banded gneiss has a low relief and lie at the south eastern part and there is occurrence of it at the western part of the study area. The rock showed evidence of tectonic reworking and has prominent strike and dips of 352°/86° W other strike and dips observed are 020°/68° W and 058°/66° E. The orientation of the intrusive bodies varies as 340°, 298°, 308°, 298°, 030° and 196°. Structurally, the banded gneiss is folded and highly fractured. The strike of the fractures varies as 130°, 240°, 325°, and 010°.

The amphibolites dominate the Central part of the study area and extend to the North Western side. The predominant strike and dip are 034°/17° W and 014°/38° W. There are evidences of

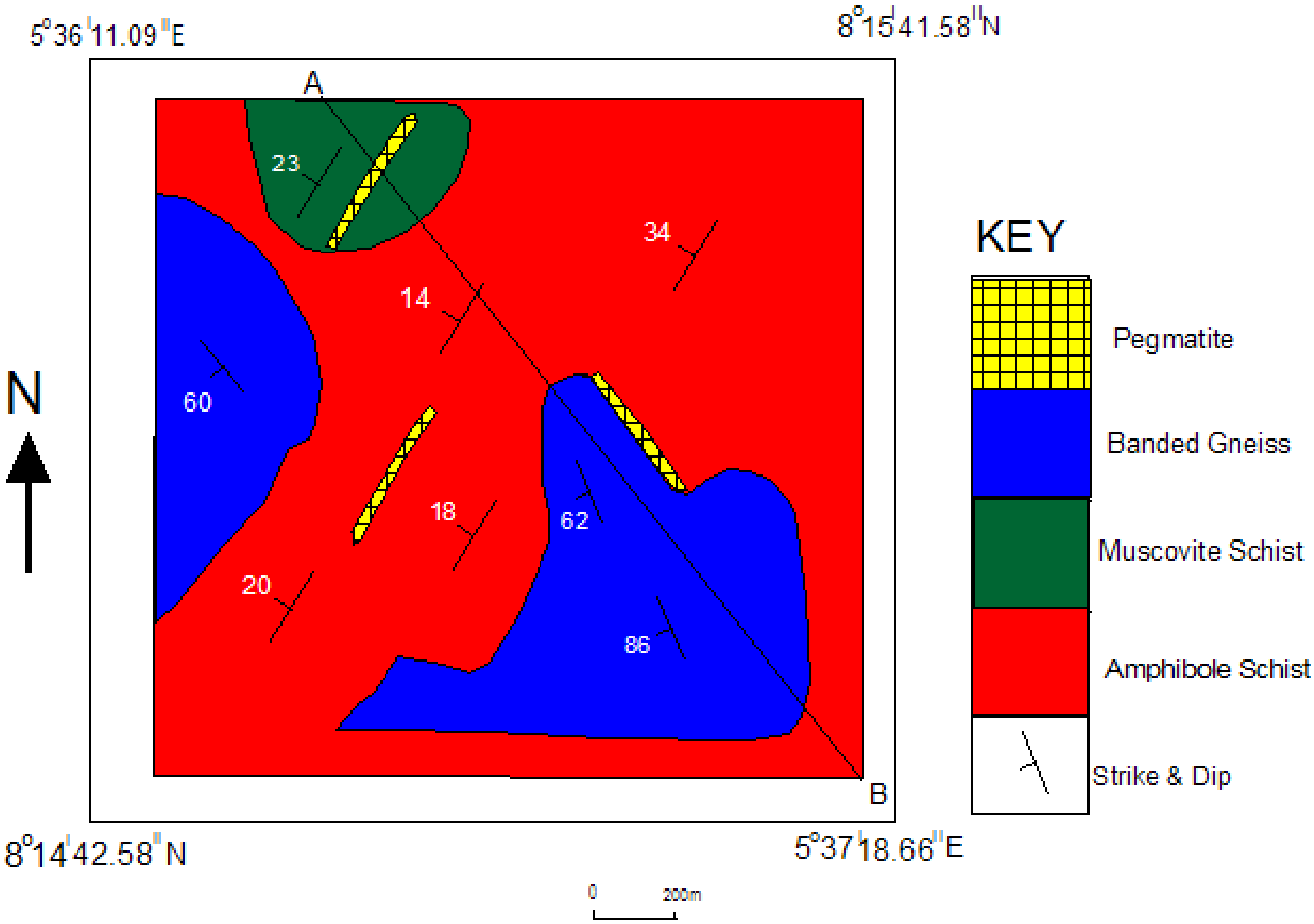

Figure 2. The geological map of Odo Ara area.

pegmatite intrusion in this area, which has strikes of 023°, 300° and 140°.

The schist occurs at the Northern part of the study area. It is striking north-easterly and dipping westerly and most of the pegmatite intrusions in this rock are intruding concordantly to the host rock. The rose diagram representing the fracture and foliation of the study area are shown in Figure 3.

Method

Sixty stations in the study area were pre selected and spaced at about 200 m apart as shown in Figure 4. These stations were arranged in profiles in such a way that each profile contains seven stations (except profiles 8 and 9 which has six stations each). At each of these stations, Radial Vertical Electrical Sounding (RVES) was carried out along three directions; 0^0, 60^0 and 120^0 and were distributed to cover the three main rock types in the area so as to observe the correlation between the measured structural directions and the plotted anisotropy polygon directions. The maximum spread of AB/2 in this area is 100 m. The results of the maximum spread, which is at current electrode spacing (AB/2) of 100 m, were used to produce the iso-resistivity map.

It is known that in any formation which is anisotropic due to the presence of fractures, the apparent resistivity (ρ_t) measured normal to its strike direction is greater than apparent resistivity (ρ_s) measured along the strike direction, when Schlumberger or Wenner array is used but contrary when crossed square array method is employed (Lane et al., 1995). A useful parameter of anisotropic medium is the co-efficient of anisotropy λ and is calculated by:

$$\lambda = \sqrt{(\rho t \,/\, \rho s)}$$

Field trials show that the anisotropic analysis not only accounts for the major part of the observed orientational variations in resistance, but also yields sounding curves of resistivity, anisotropy and strike, which vary systematically with electrode spacing.

The apparent resistivity was measured along three different azimuths N-S, NE-SW and NW-SE for a given AB/2 separations and were plotted along their corresponding azimuths. Lines of the resistivity of the same value along different azimuths were joined together, thus resulting in a polygon. A set of such polygons obtained corresponding to different AB/2 separations is known as a polar diagram or anisotropy polygon. For an isotropic homogeneous formation, this polygon will assume a circular shape. Any deviation from a circle to an ellipse is indicative of anisotropic nature of the formation (Mallik et al., 1983). The major or longest axis of the ellipse, which can fit any of such anisotropic polygons, gives the strike direction of the fracture. The co-efficient of apparent anisotropy (λa) (designated here as the degree of fracturing) is calculated from each anisotropy ellipse (fitted through each polygon) using the relationship $\lambda a = a / b$, where a and b

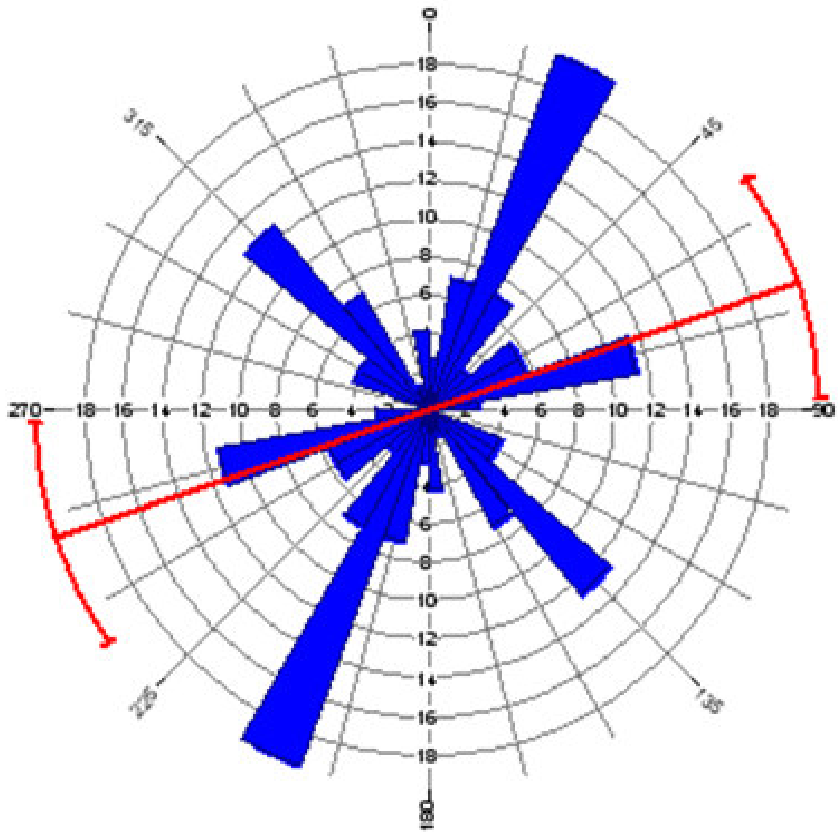

Figure 3. The rose diagram of the foliations of Odo Ara study area.

are the semi major and semi minor axes of the element. All the calculated λa values are then plotted against the corresponding AB/2 separations. The behaviour of rock fracturing at various depth equivalents to different AB/2 separations can thus be understood qualitatively from the variation of λa (Habberjam, 1975).

From the 60 RVES survey carried out, the apparent resistivity anisotropy polygon was plotted and coefficient of anisotropy was calculated for each station, using the methods of Habberjam (1972, 1975, 1979), Lane et al. (1995), Mallik et al. (1983), Olasehinde (1984), and Okurumeh and Olayinka (1998).

The data obtained were plotted against the electrode spacing on bilogarithm coordinates and a preliminary interpretation was carried out using partial curves matching involving two-layer master curves and the appropriate auxiliary charts of Rijkswaterstaat (1975). The layered earth model thus obtained, served as input for an inversion algorithm, WINRESIST, as a final stage in quantitative data interpretation. The reflection coefficients (r) of the study area were calculated using the method of Olayinka (1996); Bhattacharya and Patra (1968) and Loke (1999):

$$r = (\rho n - \rho (n-1)) / (\rho n + \rho (n-1))$$

Where ρn is the layer resistivity of the nth layer and ρ (n-1) is the layer resistivity overlying the nth layer.

RESULTS AND DISCUSSION

The result of the RVES data for the study area were plotted and interpreted. A typical graphical plot of RVES at stations 4 and 6 is shown in Figure 5 and the geometry of the curves showed that the effect of anisotropy is evident in these results, as the values of resistivity are changing with direction. It also revealed that the curves are predominantly made up of three layers of H-type (that is, $\rho1 > \rho2 < \rho3$), where ρ1, ρ2, ρ3 are the resistivity of the first, second and third layer respectively. The remaining curves are four to five layers of QH ($\rho1 > \rho2 > \rho3 < \rho4$), HA ($\rho1 > \rho2 < \rho3 < \rho4$) and HKH ($\rho1 > \rho2 < \rho3 > \rho4 < \rho5$). Their relative occurrence was represented by a pie chart shown in Figure 6.

The isopach map of the area which is the thickness of the overburden (depth to basement) is presented in Figure 7. The shallow part is at the centre of the area while the deepest part in the area is at the south-eastern and northern part of the study area.

The result of the iso-resistivity map is shown in Figure 8 and shows a considerable agreement with the geology of the area. The schist and the amphibolites could not be distinctly differentiated on the basis of resistivity values because they are both characterized by low resistivity values.

The low resistivity value which is less than 150 Ωm is the characteristic of the central part of the map and corresponds to the area occupied by the amphibolite

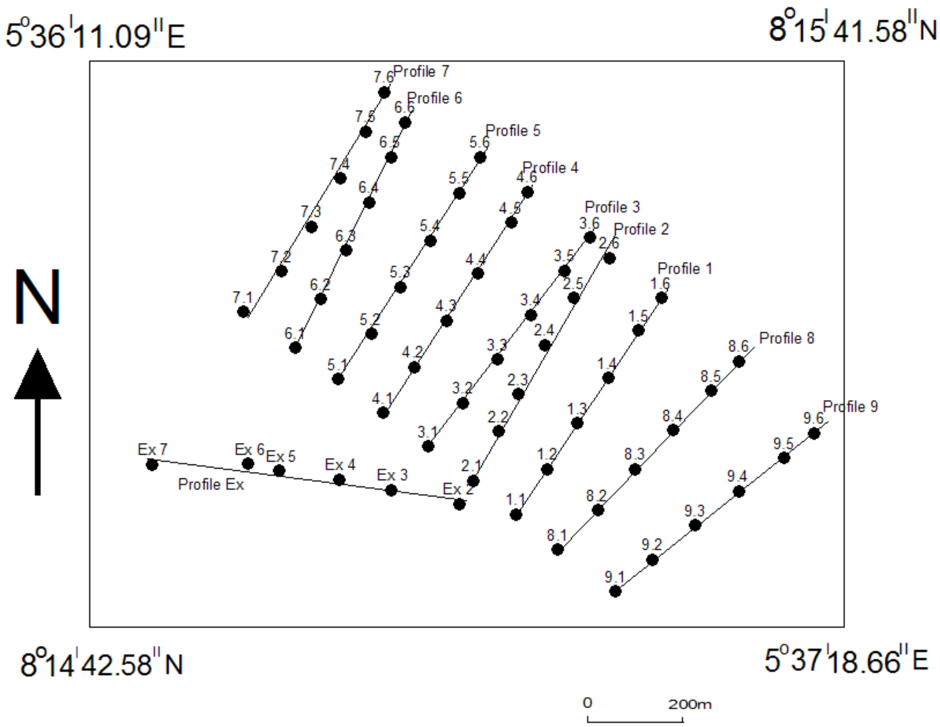

Figure 4. The layout of Odo Ara RVES survey points.

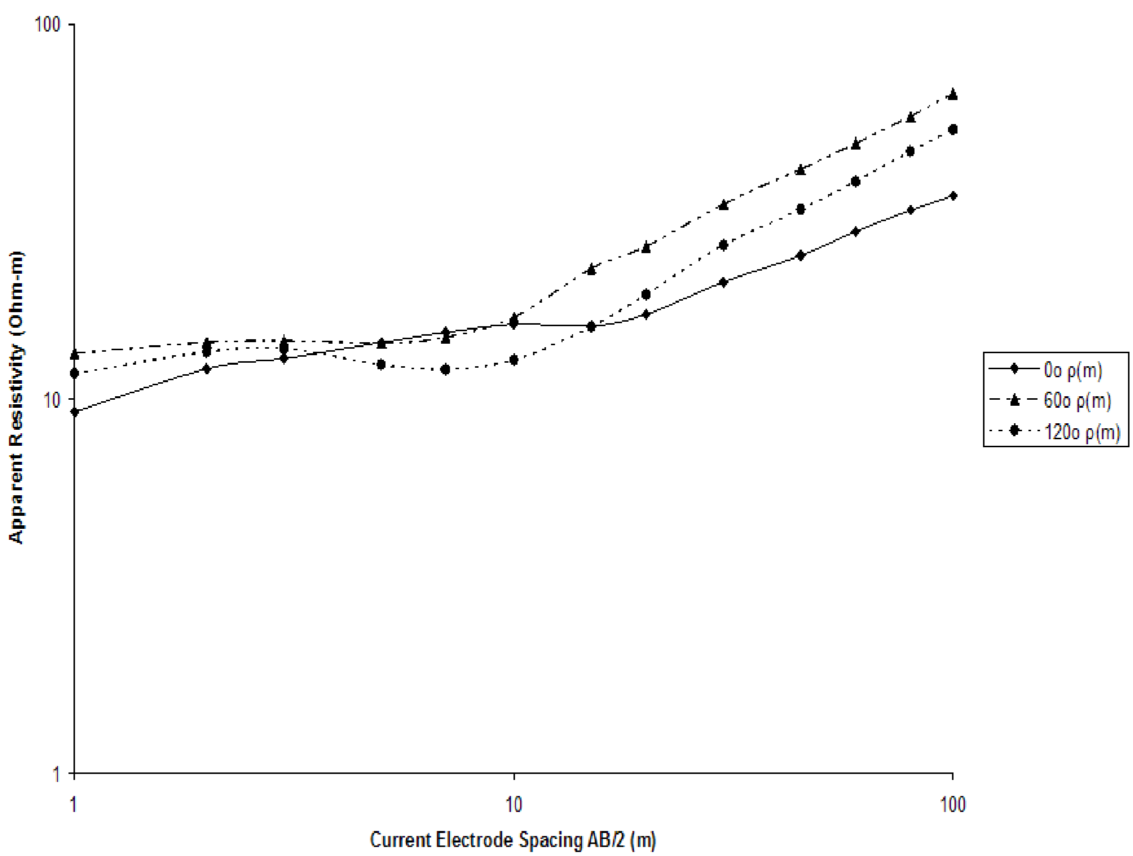

Figure 5. Typical RVES curve of Station 4,6 in the study area.

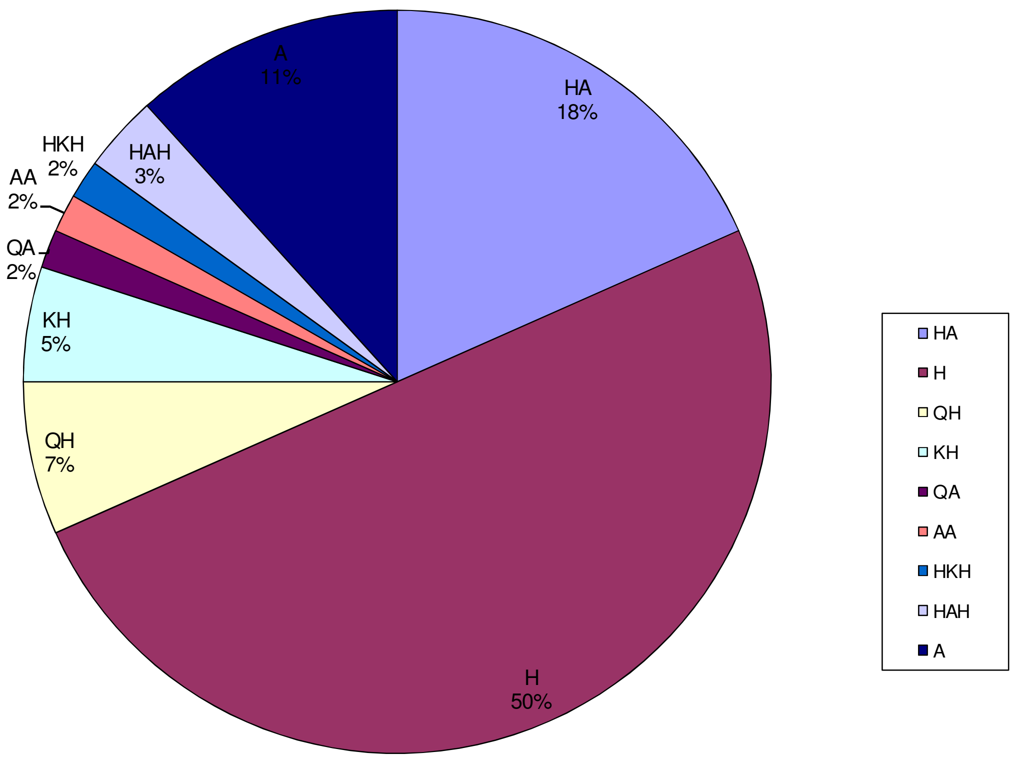

Figure 6. The pie chart showing the types of VES curves in the study area.

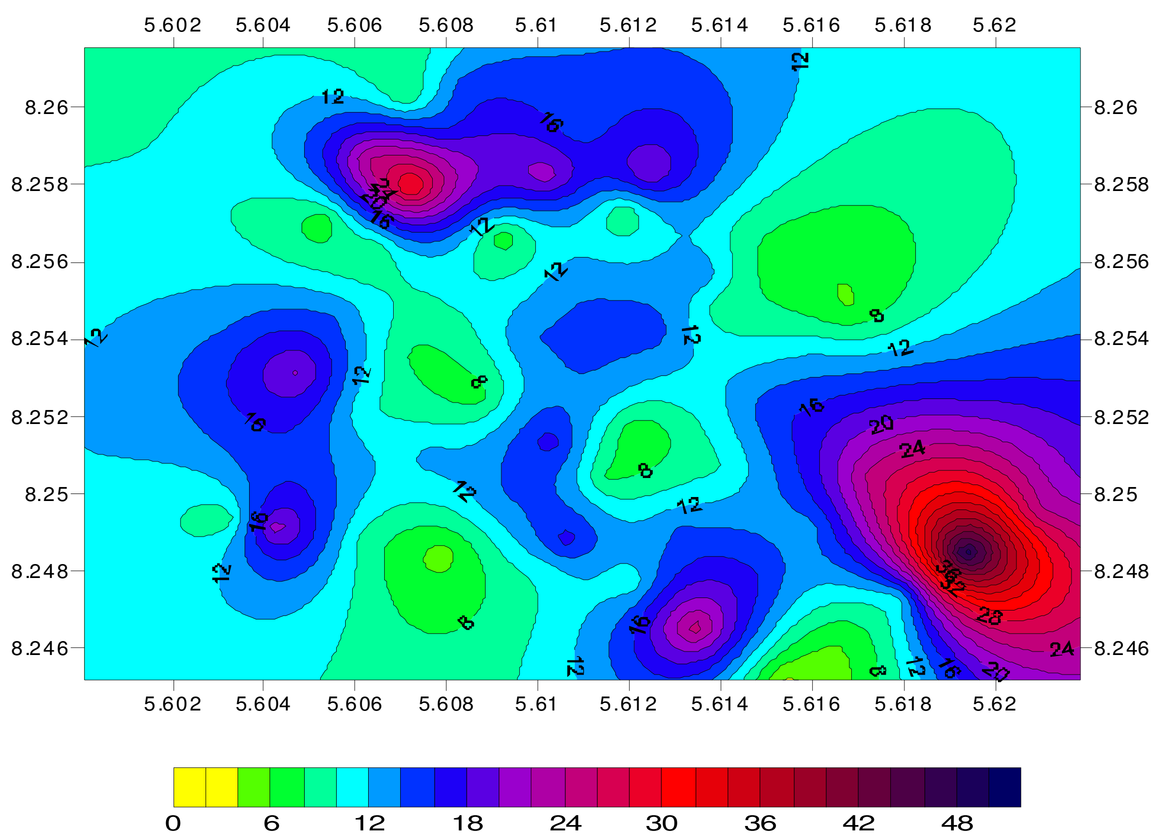

Figure 7. The isopach map of the overburden in the study area.

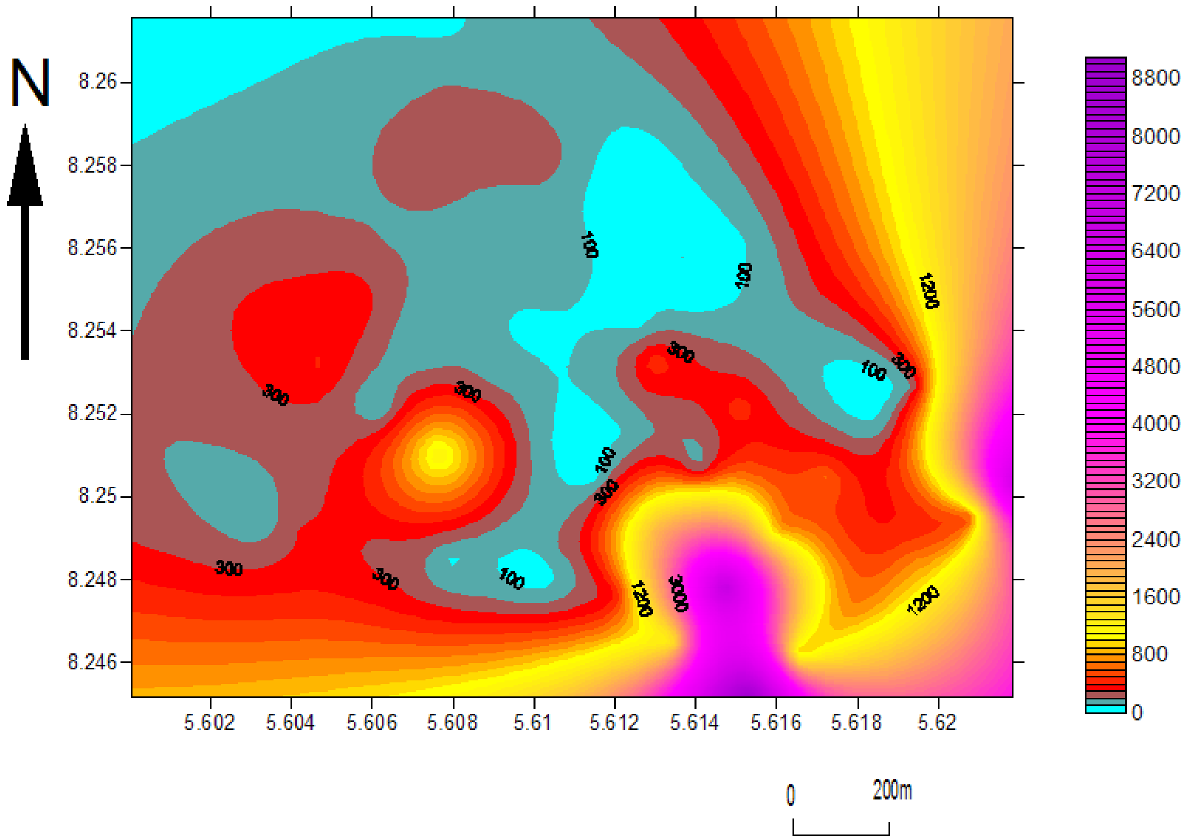

Figure 8. The iso-resistivity map of the study area produced from the iterated resistivity data.

schist rocks. Resistivity values higher than 150 Ωm characterised the eastern part of the map and some part of the west which corresponds to the area occupies by banded gneiss. The high resistivity values on the map, trending NW-SE at the south-eastern part of the map corresponds to the pegmatite intrusion in the area. However, relatively high resistivity values are observed at the north-eastern and south-eastern part of the map known to be dominated by amphibolites, this might be as a result of the influence of quartz and pegmatite intrusion, which is prominent in this area. This shows the non-uniqueness of the resistivity measurement (Olayinka, 1996). However, the resistivity pseudosections of profiles 1, 2, and 8 are presented in Figures 9 to 11 and shows agreement with the geology of the area. It reveals the interrelationship of the resistivity characteristics of the subsurface along a profile and helps to resolve areas where the geology could not be ascertained as a result of thick overburden in the area. In Profile 1, the high resistivity values at station 1, 4 mark the resistive body of pegmatite intrusion within the low resistive body of amphibolite. Profile 2 shows the plot of pseudo section on an area with the same rock unit of amphibolites which has resistivity of less than 150 Ωm. Profile 8 reveals relatively high resistivity values of banded gneiss which occupies the area but the resistivity values towards the NE, that is, at 8, 5 and 8, 6 is of lower resistivity of the amphibolite, therefore the boundary can be inferred to be between 8, 4 and 8, 5. This reveals more than one lithologic unit in the area. Pseudo section across section 1 plotted showed the variation of the resistivity values as a result of more than one lithologic unit in the area. The south eastern part, that is, at station 9, 1 and 8, 1which is characterised by high resistivity reveal the banded gneiss and the low resistivity values towards the centre reveal the amphibolite.

The iterated curves plotted for the direction of 0° along the profile lines were used to produce the geoelectric section. The geoelectric section along profile line 1 (Figure 13) revealed that the line is made up of three layers; the first layer is the resistivity top soil and has resistivity range of 218 to 1122 Ωm and a thickness range of 0.7 to 1.2 m, having relatively higher thickness at station 1,4. The second layer is the clayey weathered rock which has resistivity range of 7.3 to 198 Ωm and a thickness range of 2.4 to 14.5 m, the thickness is high at stationsm 1,2 and 1,4 and relatively shallow at station 1,6. The third layer which is to infinity, as revealed by the calculation of the reflection coefficient is the fractured /fresh basement rock and has resistivity range of 124 to 11960 Ωm. The geoelectric section along profile line 2 (Figure 14) revealed that the line is made up of two

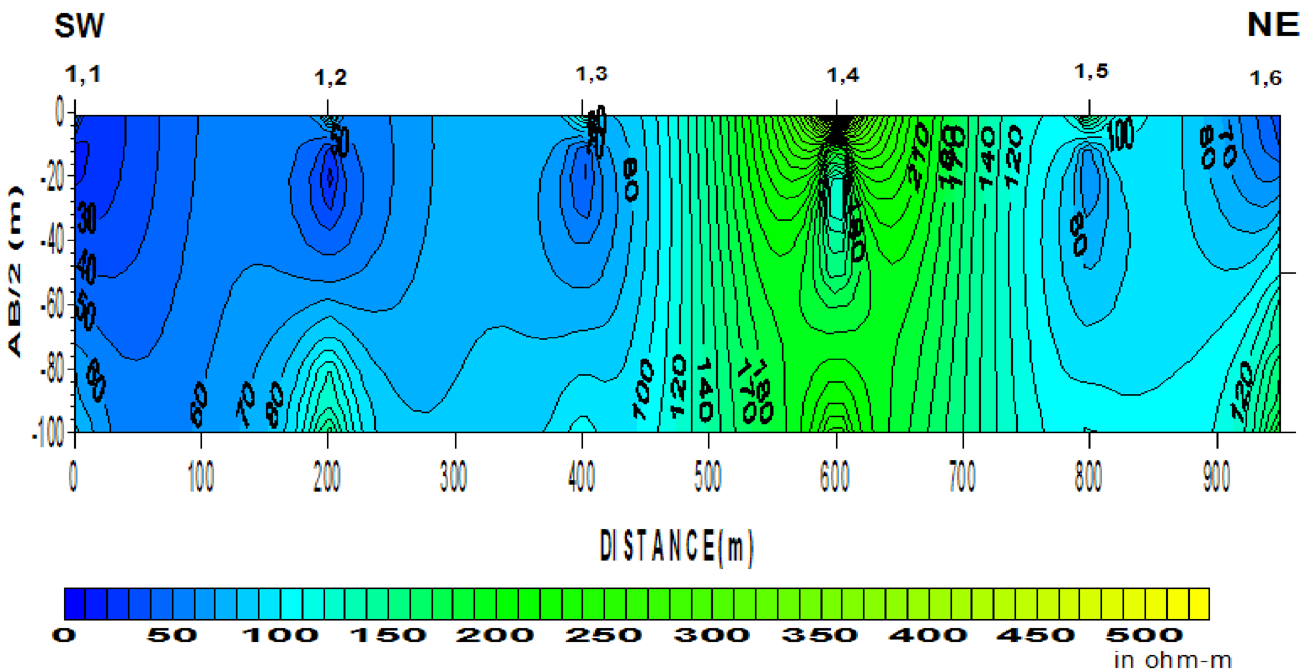

Figure 9. The pseudosection for profile 1 of Odo Ara study area.

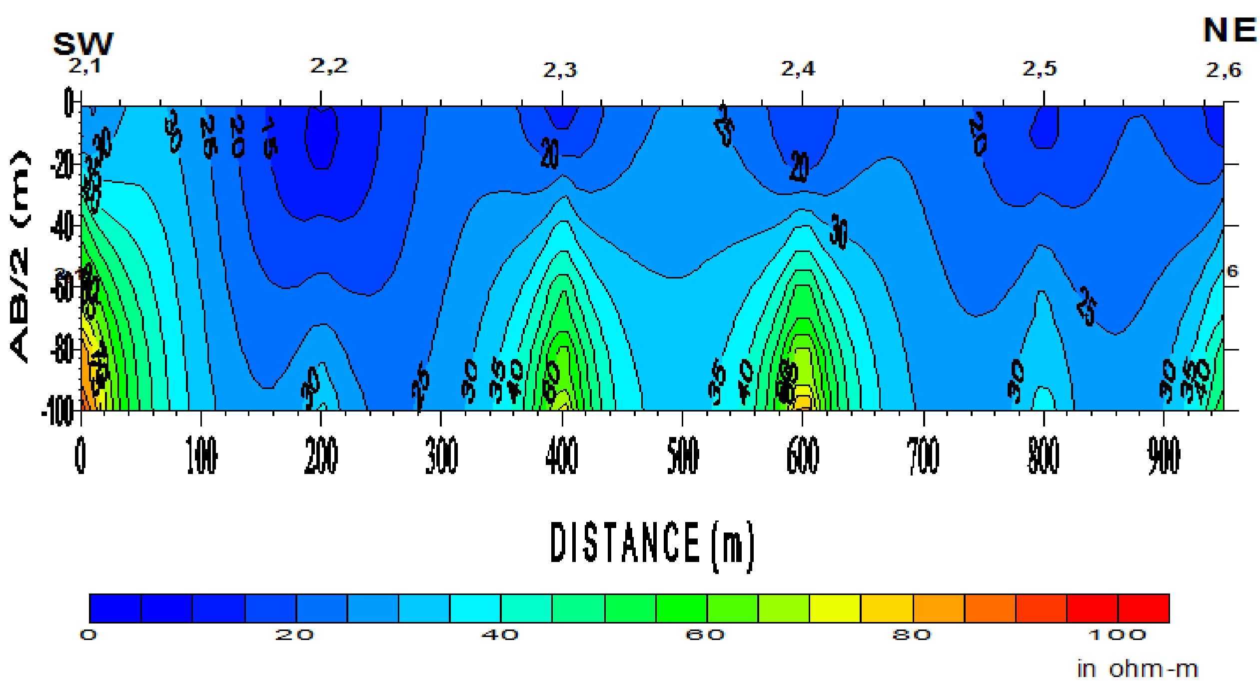

Figure 10. The pseudosection for profile 2 of Odo Ara study area.

layers; the first layer is the conductive clayey weathered rock and has resistivity range of 3 to 91 Ωm and a thickness range of 6.4 to 12.5 m and it is thicker at station 2,1 and 2,4, while the second layer is the infinite fractured basement rock and has resistivity range of 44 to 473 Ωm.

The geoelectric section along profile line 8 (Figure 15) revealed that the line is also made up of three layers the first layer is the thin resistive top soil, which is absent at the NE end of the profile line (which is at station 8,6), it has resistivity range of 137 to 1583 Ωm and a thickness

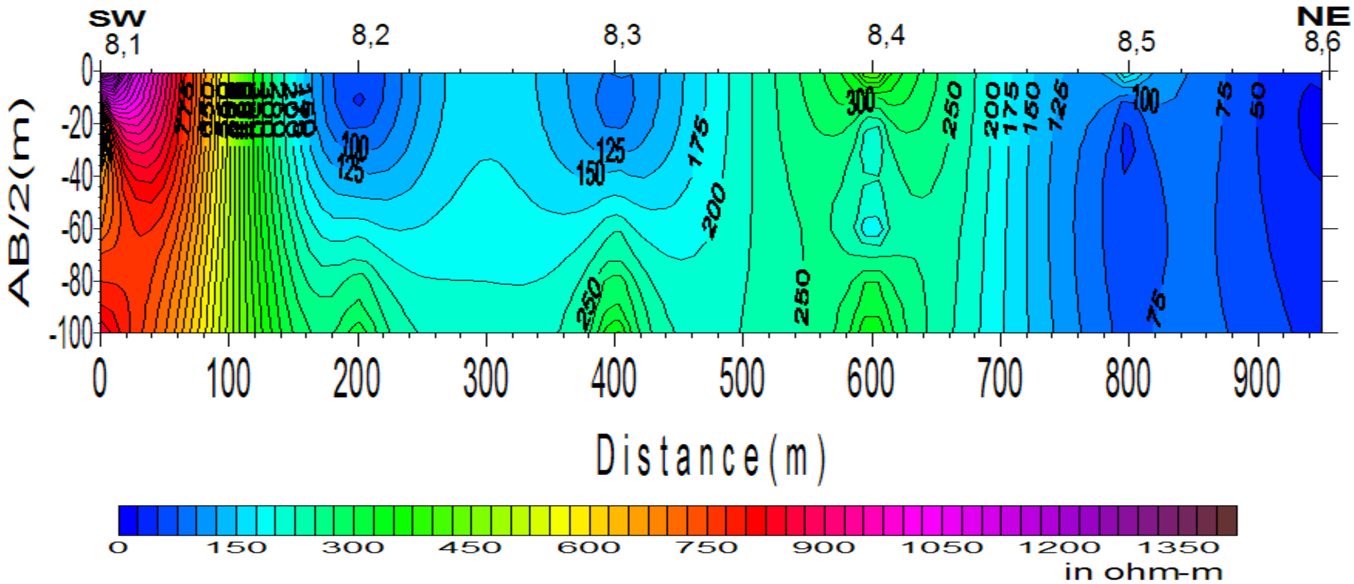

Figure 11. The pseudosection for profile 8 of Odo Ara study area.

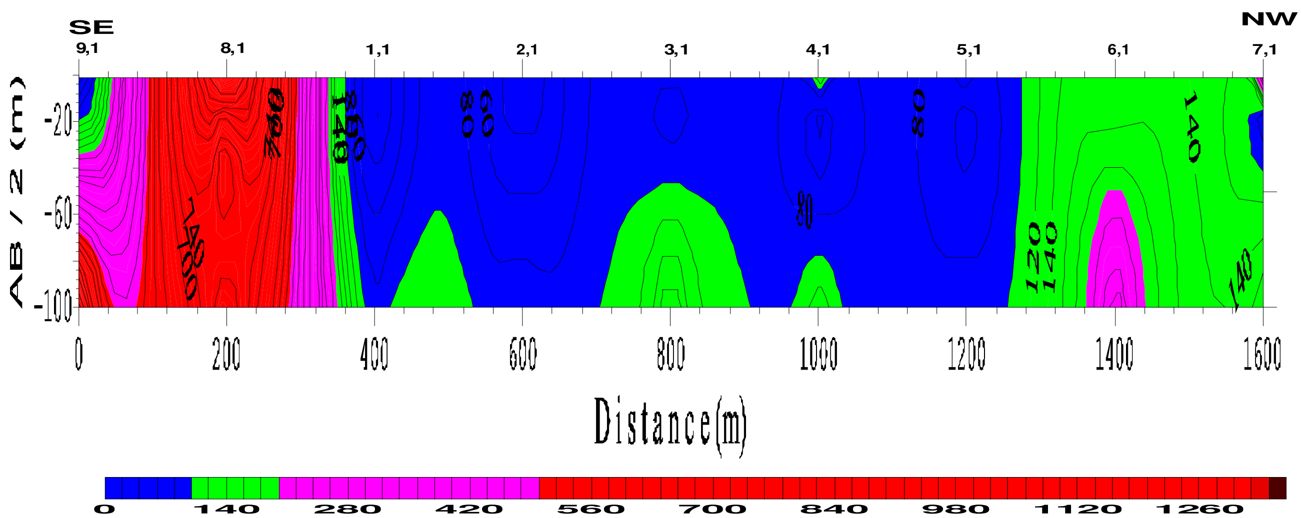

Figure 12. The pseudosection for section 1 of Odo Ara study area.

range of 0.5 to 6.8 m,. The second layer is interpreted as the weathered rock with lower resistivity value, it has resistivity range of 218 to 1122 Ωm and a thickness range of 12.1 to 20.5 m, the thickness is higher at stations 8,1 and 8,5 and relatively shallow at station 8,2. The third layer which is to infinity also suggests a fresh basement rock and has resistivity range of 197 to 7015 Ωm.

The reflection coefficient map of the area is plotted and presented in Figure 16. Olayinka (1996) observed that an area of lower reflection coefficient value exhibits a weathered or fracture of its basement rock, thus, has a higher water potential. It therefore measures the degree of fracture of an area.

The anisotropy polygon directions of the 60 stations are presented in Table 1 and reveal that the area dominated by banded gneiss has a dominant structural trend of NW-SE direction. The areas occupied by amphibolite and schist are dominated by NE-SW.

However, the amphibolite and schist could not be separated on the basis of anisotropy polygon direction; this is as a result of the two rock units having the same geologic foliation direction. The anisotropy polygon plotted for stations 5,1 and 9,2 are presented in Figures 17 and 18 respectively.

It is interesting to note that the deepest part of the isopach map (at the south-eastern part) corresponds to

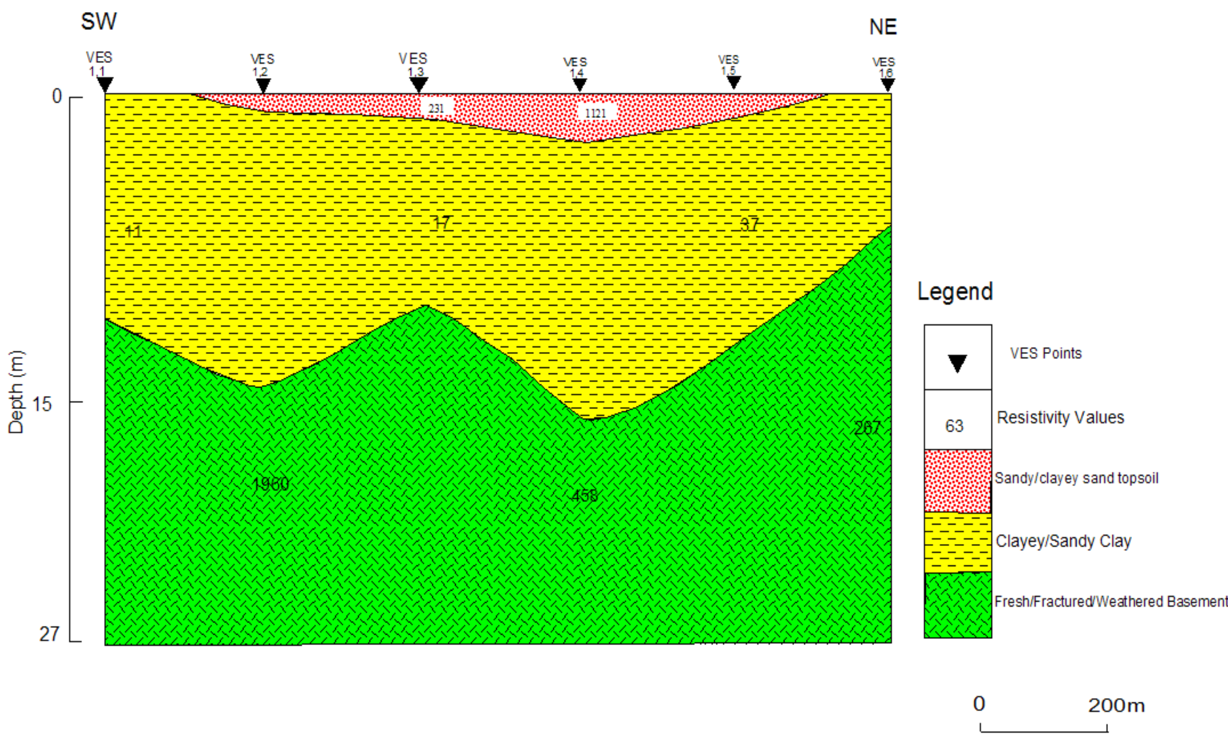

Figure 13. The geoelectric section for profile 1 of the study area.

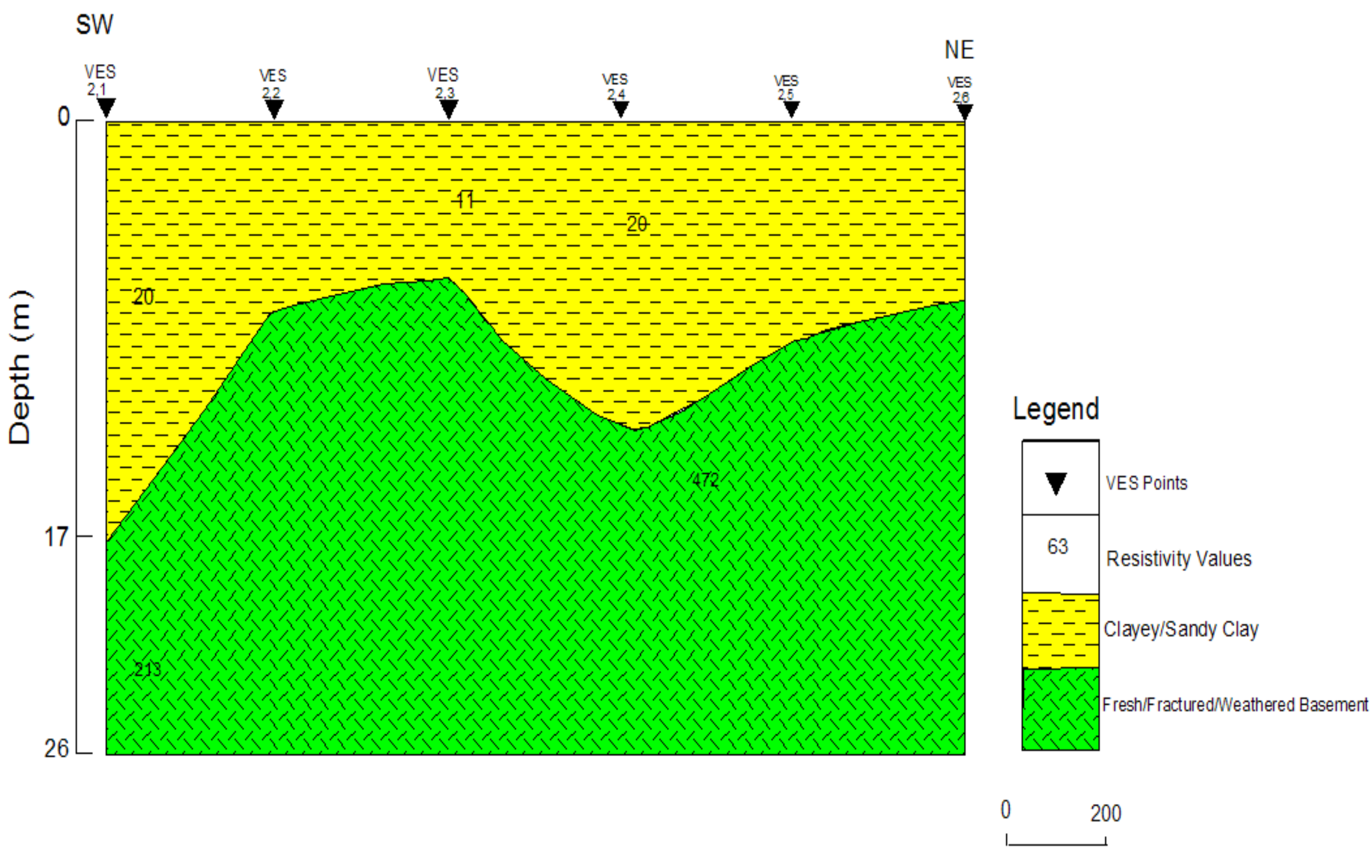

Figure 14. The geoelectric section for profile 2 of the study area.

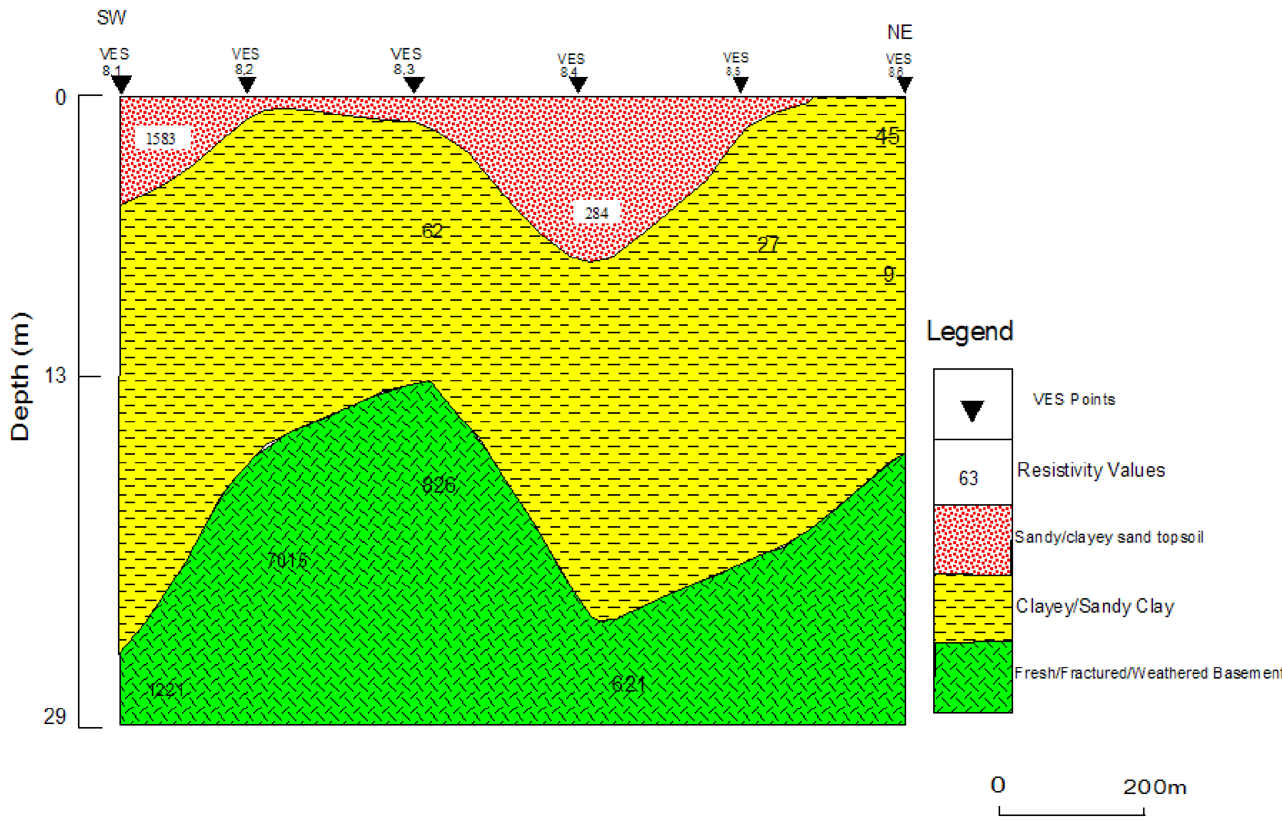

Figure 15. The geoelectric section for profile 8 of the study area.

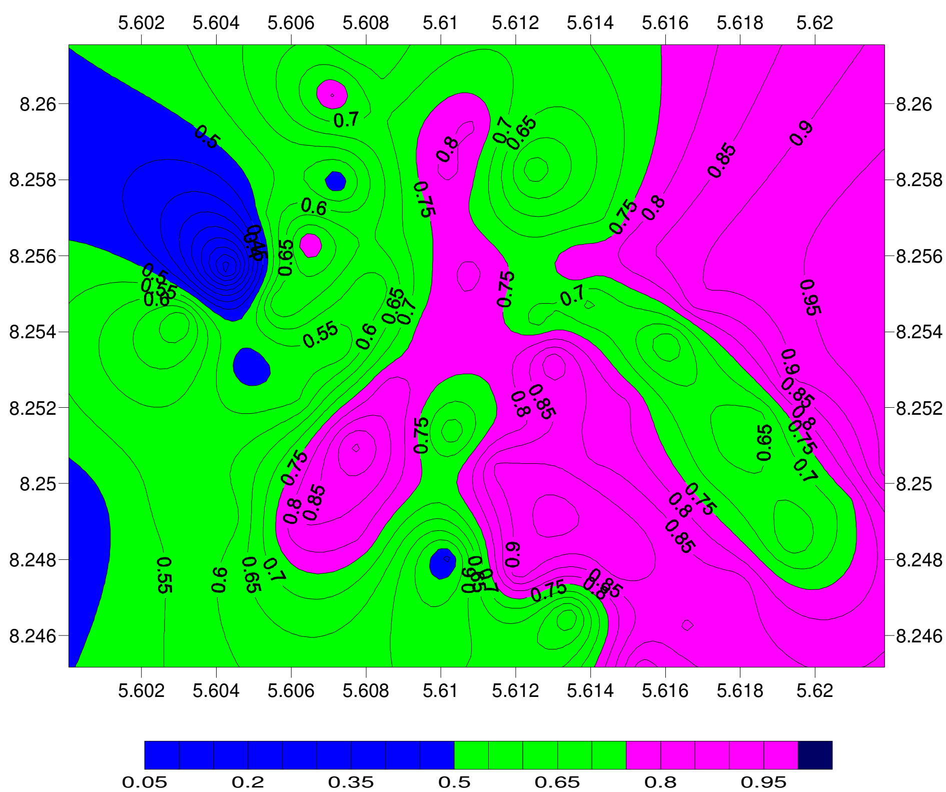

Figure 16. The reflection coefficient map of the study area.

Table 1. Table showing the anisotropy polygon directions of all the stations in the study area and their corresponding geology.

Station	Anisotropy polygon direction	Geology	Station	Anisotropy polygon direction	Geology
1,1	NE	Amphibolite	6,1	NW	Banded Gneiss
1,2	NE	Amphibolite	6,2	NE	Amphibolite
1,3	NE	Amphibolite	6,3	NNE	Amphibolite
1,4	NW	Pegmatite	6,4	NW	Banded Gneiss
1,5	NE	Amphibolite	6,5	NW	Banded Gneiss
1,6	NE	Amphibolite	6,6	NW	Banded Gneiss
2,1	NE	Amphibolite	7,1	NW	Banded Gneiss
2,2	NNE	Amphibolite	7,2	NW	Banded Gneiss
2,3	NEE	Amphibolite	7,3	NWW	Banded Gneiss
2,4	NW	Amphibolite	7,4	NW	Amphibolite
2,5	NE	Amphibolite	7,5	NW	Amphibolite
2,6	NE	Amphibolite	7,6	NE	Amphibolite
3,1	NE	Amphibolite	8,1	NW	Banded Gneiss
3,2	NE	Amphibolite	8,2	NW	Banded Gneiss
3,3	NNE	Amphibolite	8,3	NW	Banded Gneiss
3,4	NE	Amphibolite	8,4	NW	Banded Gneiss
3,5	NE, NEE	Amphibolite	8,5	NE	Amphibolite
3,6	NW	Amphibolite	8,6	NW	Banded Gneiss
4,1	NNE, NE	Amphibolite	9,1	NW, NWW	Banded Gneiss
4,2	NEE	Amphibolite	9,2	NW	Banded Gneiss
4,3	NE	Amphibolite	9,3	NEE	Amphibolte
4,4	NE	Amphibolite	9,4	NW	Banded Gneiss
4,5	NE	Amphibolite	9,5	NE	Amphibolte
4,6	NW	Amphibolite	9,6	NE	Amphibolte
5,1	NEE	Amphibolite	Ex 2	NE	Amphibolte
5,2	NEE	Amphibolite	Ex 3	NE	Amphibolte
5,3	NE	Amphibolite	Ex 4	NE	Amphibolte
5,4	NE	Amphibolite	Ex 5	NW	Banded Gneiss
5,5	NE	Amphibolite	Ex 6	NW	Banded Gneiss
5,6	NE	Amphibolite	Ex 7	NW	Banded Gneiss

the area of high resistivity values. Although a fairly low bedrock resistivity is generally indicative of the probable presence of fractured bedrock, the situation may be complicated by the non-uniqueness of the bedrock resistivity.

All the maps produced from the interpretation of the RVES data, that is, isopach, resistivity, reflection coefficient and anisotropy coefficient maps, reveal a NE-SW directional trend in the area occupied by the banded gneiss, most especially at the south-eastern part of the study area.

A geological map was inferred and produced based on the interpretation of the electrical resistivity data and is presented in Figure 19. The map shows high agreement with the field geologic map of the area. However, some parts of the area known to be dominated by amphibolites especially at the north-eastern and south-western part of the study area are mapped as banded gneiss. This is because these areas have been highly intruded by resistive quartz veins and pegmatites. The superposition of anisotropy polygon direction on this inferred geologic map resolved these controversial areas. The controversial area at the south-western part shows a NE-SW anisotropy direction of amphibolite gneiss, which corresponds to the field geology of the area.

Conclusion

The study area, Odo Ara, West Central Nigeria was investigated using RVES techniques. The amphibolite and schist are characterised by low resistivity of less than 100 Ωm while the banded gneiss has higher resistivity of greater than 100 Ωm. The resistivity parameters showed that the amphibolite and schist has NE – SW anisotropy direction, the banded gneiss has NW – SE direction, and

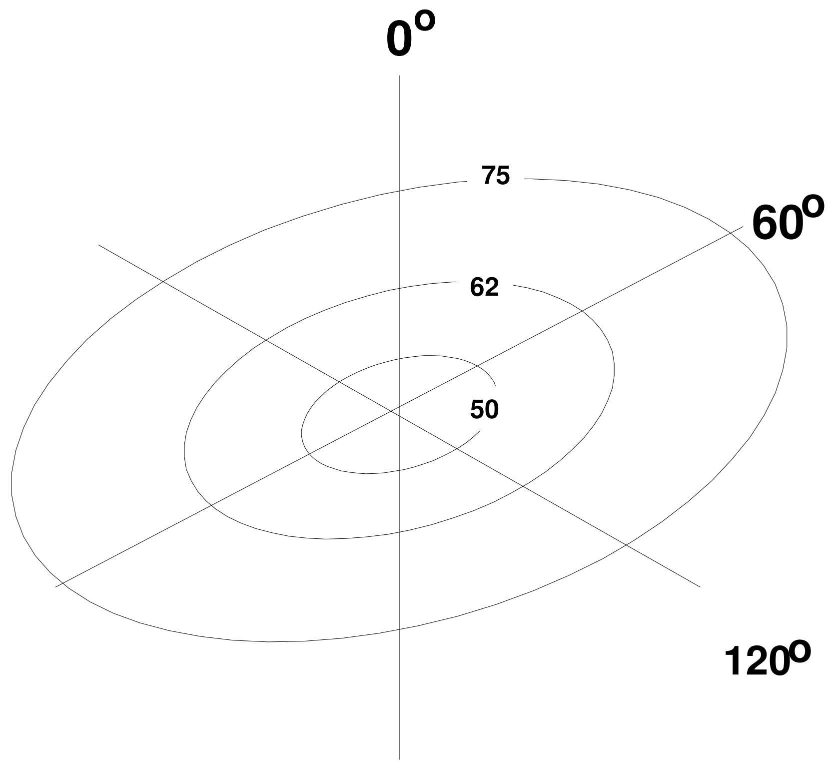

Figure 17. The anisotropy polygon of station 5,1 of the study area.

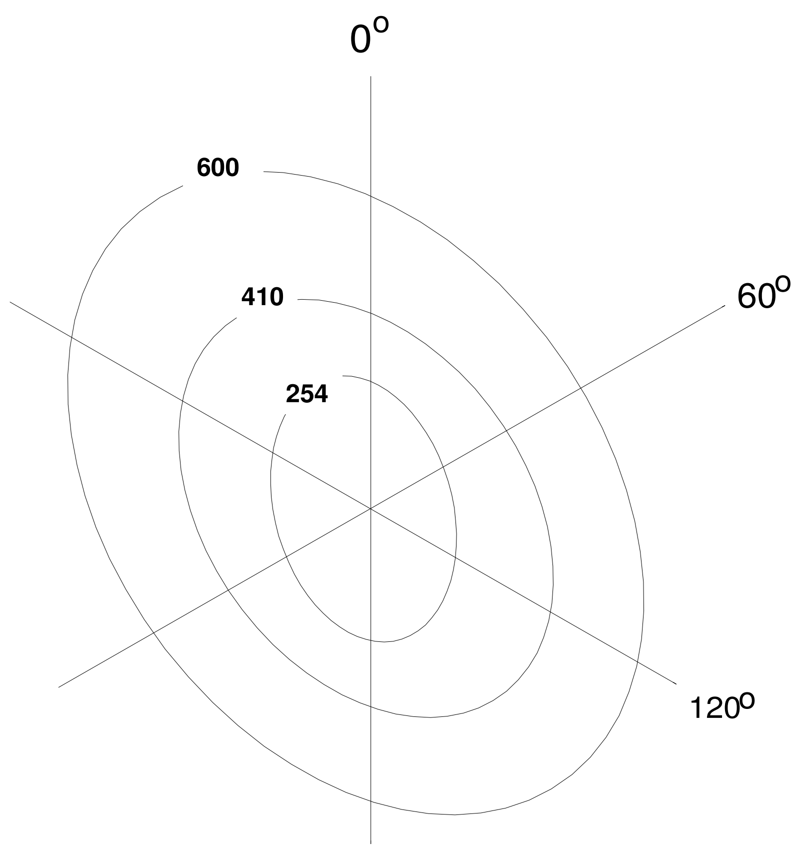

Figure 18. The anisotropy polygon of station 9,2 of the study area.

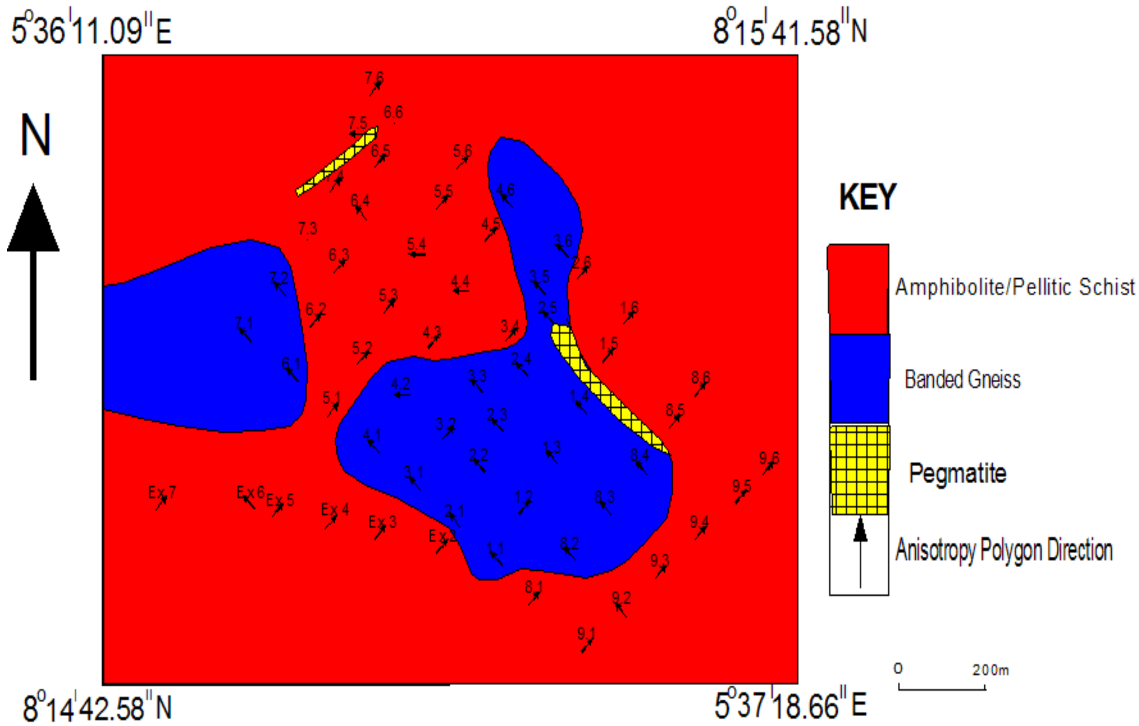

Figure 19. The geological map produced from the superposition of the anisotropy directions and the resistivity map of Odo Ara.

this also agrees significantly with the geology of the area. However, the combination of the anisotropy polygon and the iso resistivity map has reduced the ambiguity inherent in using a single geophysical parameter.

REFERENCES

Annor AE, Olasehinde PI, Pal PC (1990). Basement fracture patterns in the control of water channels. An example from Central Nigeria. J. Min. Geol., 26(1): 5-11.

Bhattacharya PK, Patra HP (1968). Direct Current Geoelectric, Sounding Methods in Geochemistry and Geophysics. Elsevier, Amsterdam, p. 135.

Dada SS, Birck JL, Lancelot JR, Rahaman MA (1993). Archaean migmatite-gneiss complex of North Central Nigeria: Its geochemistry, petrogenesis and crustal evolution. Int. Colloguiom Afr. Geol., Mbabane, Swaziland, 1: 97-102.

Dada SS (2006). Proterozoic Evolution of Nigeria. In: O. Oshin (Ed). The Basement Complex of Nigeria and its Mineral Resources. M.A.O. Rahaman Symposium, pp. 29-44.

David LM (1994). Ambiguities in VES interpretation: Case histories in southern Nigeria. Water Resour., 4(1&2): 43-48.

Eduvie MO (1991). Groundwater Investigation, Assessment and Borehole Design and Completion in the Basement Complex Area: Kaduna sheet 123 SE. Unpub. M. Sc. Thesis, Dept. of Geology, Ahmadu Bello University, Zaria, Nigeria, p. 131.

Habberjam GM (1972). The effects of Anisotropy on Square Array Resistivity Measurements. Geophys. Prospect., 23: 211-247.

Habberjam GM (1975). Apparent Resistivity Anisotropy and Strike measurements. Geophys. Prospect., 23: 211-215.

Habberjam GM (1979). Apparent Resistivity Observation and the Use of Square Array Techniques. In: Saxov, S and Flathe, H. (eds). Geoexplor. Monogr. Ser., 1(9): 211-247.

Lane JW Jr., Haeni FP, Waston WM (1995). Use of a Square-Array Direct-Current Resistivity Method to detect Fractures in Crystalline Bedrock in New Hampshire. Ground Water, 33(3): 476-485.

Loke MH (1999). Electrical Imaging surveys for environmental and engineering studies. A practical guide to 2-D and 3-D surveys. Terraplus Inf., p. 67.

Loke MH, Barker RD (1996). Practical techniques for 3D resistivity surveys and data inversion. Geophys. Prospect., 44: 499-523.

Mallik SB, Bhattacharya DC, Nag SK (1983). Behavior of Fractures in Hard Rocks-a Study by surface geology and radial VES method. Geoexploration, 21(3): 181-189.

Okunlola OA (1998). Speciality metal potentials of Nigeria. Proceedings of 1st Minning in Nigeria Conference. Federal Ministry of Solid Minerals, Abuja, Nigeria.

Okurumeh OK, Olayinka AI (1998). Electrical Anisotropy of crystalline Basement Rocks around Okeho, southwestern Nigeria: Implications in Geologic Mapping and Groundwater Investigation. Water Resour. J. NAH, 9: 41-50.

Olasehinde PI (1984). A Comparison of Radial Geoelectrical Sounding and Structural Lineaments in the UnIlorin Main Campus. Unpublished M.Sc. thesis, University of Ilorin, Nigeria, p. 164.

Olayinka AI (1996). Non Uniqueness in the Interpretation of Bedrock Resistivity from Sounding Curves and its Hydrological Implications. Water Resour. J. NAH, 7(1&2): 55-60.

Olayinka AI (1999). Advantage of Two-Dimensional Geoelectric Imaging for Groundwater Prospecting: Case Study from Ira, Southwestern Nigeria. Water Resour. J. NAH, pp. 55-60.

Olorunfemi MO, Okhue ET (1992). Hydrogeologic and Geologic significant of a Geoelectric survey at Ile-Ife, Nigeria. J. Min. Geol., 28(2): 221-229.

Rijkswaterstaat (1975). Standard Graphs for Resistivity Prospecting. E.A.E.G., pp. 75-89.

Zohdy AA (1974). Application of Surface Geophysics to Groundwater Investigation. Techniques of water resources investigations of the US Geological Survey, Book 2, pp. 5-66.